



# Eikonal Quasinormal Modes, Photon Sphere and Shadow of a Charged Black Hole in the 4D Einstein-Gauss-Bonnet Gravity

Jose Miguel Ladino<sup>1</sup> · Eduard Larrañaga<sup>1</sup>

Received: 25 May 2023 / Accepted: 2 August 2023 / Published online: 25 September 2023  
© The Author(s) 2023

## Abstract

In this work, we investigate the relationship between the geometrical properties, the photon sphere, the shadow, and the eikonal quasinormal modes of electrically charged black holes in 4D Einstein-Gauss-Bonnet gravity. Quasinormal modes are complex frequency oscillations that are dependent on the geometry of spacetime and have significant applications in studying black hole properties and testing alternative theories of gravity. Here, we focus on the eikonal limit for high frequency quasinormal modes and their connection to the black holes geometric characteristics. To study the photon sphere, quasinormal modes, and black hole shadow, we employ various techniques such as the Wentzel-Kramers-Brillouin method in various orders of approximation, the Poschl-Teller potential method, and Churilova's analytical formulas. Our results indicate that the real part of the eikonal quasinormal mode frequencies of test fields are linked to the unstable circular null geodesic and are correlated with the shadow radius for a charged black hole in 4D Einstein-Gauss-Bonnet gravity. Furthermore, we found that the real part of quasinormal modes, the photon sphere and shadow radius have a lower value for charged black holes in 4D Einstein-Gauss-Bonnet gravity compared to black holes without electric charge and those of static black holes in general relativity. Additionally, we explore various analytical formulas for the photon spheres and shadows, and deduce an approximate formula for the shadow radius of charged black holes in 4D Einstein-Gauss-Bonnet gravity, based on Churilova's method and its connection with the eikonal quasinormal modes.

**Keywords** Quasinormal modes · Einstein-gauss-bonnet gravity · Black hole shadow · Photon sphere

---

✉ Jose Miguel Ladino  
jmladinom@unal.edu.co

Eduard Larrañaga  
ealarranaga@unal.edu.co

<sup>1</sup> Universidad Nacional de Colombia. Sede Bogotá. Facultad de Ciencias. Observatorio Astronómico Nacional, Ciudad Universitaria, Bogotá, Colombia

## 1 Introduction

Modified gravity theories have gained attention as a potential solution to various unresolved astrophysical mysteries, including the nature of dark matter, the formation of supermassive Black Holes (BHs), the evolution of galaxies, and the behavior of large-scale structures in the universe, as well as the acceleration of its expansion. One of these theories is known as the Einstein-Gauss-Bonnet (EGB) gravity, which introduces the Gauss-Bonnet invariant as an additional term to the Lagrangian. This theory of gravity can be interpreted as an extension of GR with quadratic curvature corrections, yielding interesting implications for BHs, cosmology, and weak-field gravity [1]. Particularly, the BH solutions in EGB gravity have been derived from various modified gravity theories using different approaches. The initial BH solution in EGB theory was found by Boulware and Deser in 1985 [2] for dimensions  $D \geq 5$ , as the GB term does not affect the gravitational dynamics in  $D = 4$ . However, later studies, such as those by Tomozawa in 2011 [3] and Cognola et al. in 2013 [4], discovered that the GB term could have a non-trivial contribution to spacetime when  $D = 4$  through regularization and dimensional reduction techniques. According to Lovelock's theorem, EGB gravity is only introduced in  $D \geq 5$ , as the GB term does not contribute dynamically in lower dimensions [5]. This led Glavan and Lin in 2020 [6] to propose a rescaling of the coupling constant to obtain a contribution to gravitational dynamics in  $D = 4$ . From this moment, this BH solution in 4D EGB gravity has been studied intensively and is considerably a subject of ongoing research. For example, this BH solution in 4D EGB theory was explored subsequently in 2020 [7] by Fernandes, who studied its coupling with both BH electric charge and anti-de Sitter space. Despite the fact that the solution proposed by BH in [6] was obtained in a simple way, the model used there was strongly criticized. Several later studies have shown that the method used to find the solution was neither consistent nor well-defined [1, 8–10]. However, several subsequent studies have obtained this same solution and clarified that it was not really new. This and other very similar solutions can be deduced from different well-defined approaches and modified gravity theories [1, 11–17].

On the other hand, remarkable progress in observational astronomy has been achieved in recent years, particularly in the study of BHs. One of the most intriguing properties of BHs is their Quasinormal Modes (QNMs), which can be detected by gravitational interferometers. These QNMs are a distinguishing characteristic of BHs that describe their damped oscillations over the spacetime in response to external perturbations [18]. These modes are fundamental to understanding the behavior of BHs and play a crucial role in verifying the theoretical predictions of gravitational wave physics through experimental measurements. The frequencies of these QNMs of BHs are complex numbers, with the real part corresponding to the frequency of the oscillation and the imaginary part corresponding to the rate at which the amplitude of the oscillation decays. QNMs have several important applications in the research of BHs, such as studying their surface gravity and horizon area, stability, the detection of gravitational waves, and their geometrical properties, such as their mass, spin, and electric charge. There are various techniques used to compute and calculate QNMs, including the Wentzel-Kramers-Brillouin (WKB) method, the continued fraction method, the time-domain integration method and much more. In Fact, the knowledge about QNMs could also have potential implications in other fields such as astrophysics, cosmology, and high-energy physics, like testing General Relativity (GR) and alternative theories of gravity [19]. Eikonal QNMs are a specific type of oscillations that are particularly useful for studying high-frequency QNMs and their applications. These oscillations occur in the eikonal limit, in which the real part of the QNM frequency is directly related to the unstable circular null

geodesics of the BH. This relationship is helpful in understanding the connection between QNMs and the geometric properties of the BH. For instance, the real part of the QNM frequency is a monotonically increasing function of the spin of the BH, whereas the imaginary part of the QNM frequency is a monotonically decreasing function of the spin. [20]. Therefore, exploring eikonal QNMs is a valuable approach to studying BHs and their geometrical properties.

Another very interesting feature of BHs is their shadow, a dark region in their vicinity caused by the bending of light due to the BHs gravity. The exact shape and size of a BHs shadow also depend on the geometrical properties of the BH, as well as the properties of the environment surrounding it, such as the distribution of matter and the presence of other objects. For example, the presence of dark matter can affect the QNMs frequencies and the shadow radius of a BH [21, 22]. The eikonal limit establishes a correlation between these two quantities, indicating that the influence of dark matter on QNMs and the shadow radius is more pronounced for rotating BHs than non-rotating ones [21].

The study of eikonal QNMs in BH solutions of GR and their connection with the photon sphere has been extensively explored in previous research [23]. These studies have also been extended to alternative theories of gravitation, such as Scalar Gauss-Bonnet gravity [24], Einstein-dilaton-Gauss-Bonnet BHs [25], dynamical Chern-Simons gravity [26], Rotating Loop Quantum BHs [27], string-corrected D-dimensional BHs [28], and deformed Schwarzschild BHs [29], among others. Additionally, the QNMs of BHs in 4D EGB gravity are a topic of ongoing research. Some investigations have focused on the shadows and photon spheres with spherical accretions, the correlation between the shadow of a BH and its eikonal QNMs, as well as the effect of the Gauss-Bonnet (GB) coupling constant  $\alpha$  on these properties [30–36]. Moreover, recent research has been conducted on extended and more complex versions of this 4D EGB BH type solution. Investigations have included the study of eikonal QNMs and greybody factors in asymptotically de Sitter spacetime [37], the investigations on the QNMs and the shadow of a BH with confining electric potential in scalar-tensor description of 4D EGB gravity [38], the effects of the magnetic charge on weak deflection angle and greybody bound of 4D EGB BHs [39], the analysis of the shadow of rotating BHs in 4D EGB gravity [40], the study of null geodesics and shadow of 4D EGB BHs surrounded by quintessence [41], the examination of entropy, energy emission, QNMs, and deflection angle of 4D EGB BHs with nonlinear electrodynamics [42], and the investigation of QNMs of a 4D EGB BH in anti-de Sitter space [43]. Similarly, several studies have been conducted on electrically charged BHs in 4D EGB gravity, each focusing on different aspects of their behavior. For instance, gravitational lensing is studied in [44], particle motion and plasma behavior are examined in [45], superradiance and stability of the solution are discussed in [46], and the connection between phase transition and QNMs is explored in [47]. Recent research has focused on the properties of rotating charged BHs in 4D EGB gravity, including the examination of photon motion and shadow [48]. Additionally, studies have been conducted on the characteristics of charged BHs in 4D EGB gravity coupled with anti-de Sitter space, such as their shadow, energy emission, deflection angle, and heat engine properties [49]. Furthermore, investigations have been carried out on the instability, quasinormal modes, and strong cosmic censorship of charged BHs in 4D EGB gravity coupled with de Sitter space under charged scalar and electromagnetic perturbations [50, 51]. Notably, by merging the findings from previous investigations, a more comprehensive understanding of these variations in modified theories of gravity can be achieved.

A recent work in [52] explored the correspondence between the shadow and the QNMs of the scalar field around a charged BH in 4D EGB gravity, using the 6<sup>th</sup> order of the WKB method. In this work, we will extend the findings of this study by utilizing additional

approaches, such as the Poschl-Teller potential and Churilova's methods, to investigate several properties that emerge the relationship between the BH shadow, and the eikonal QNMs of scalar and electromagnetic field perturbations for a charged BH in 4D EGB gravity. Therefore, We will show several new analytical formulas for the radius of the photon sphere and the BH shadow, which can be very useful because of its short form and which result from the relationship of these quantities with the eikonal QNMs.

This paper is organized as follows: In Section 2, we present the electrically charged BH in 4D EGB gravity, briefly introducing the BH metric background, their horizons, and particular limit cases. In Section 3, we show the theory behind the QNMs of scalar and electromagnetic field perturbations, providing the corresponding master wave equations and discussing some of the principal semi-analytical methods to calculate the QNM frequencies, such as the WKB approximation approach and the Poschl-Teller potential method. Then, in Section 4, we discuss some eikonal QNMs approaches, including a recently proposed analytical formulation that approximates the frequencies at this limit. Later, we analyze and apply these methods on the eikonal QNMs of a charged BH in 4D EGB gravity, looking at the effect of the geometric parameters of the BH on these. Afterwards, in Section 5, we study the photon sphere of a charged BH in 4D EGB gravity and its particular limit cases, illustrating the correspondence between eikonal QNMs and null geodesics, and revealing the effect of the geometric parameters of the BH on this. Thereafter, in Section 6, we investigate the shadow of a charged BH in 4D EGB gravity and its connection with their eikonal QNMs frequencies, sharing an analytic and approximate formula for the shadow and comparing it with all the results given by other methods and again, the effect of the geometric parameters of the BH in their shadow. Finally, in Section 7, we summarize some conclusions.

## 2 The Charged Black Hole in the 4D Einstein-Gauss-Bonnet Gravity

### 2.1 The Spacetime Background

The gravitational theory of EGB in  $D$ -dimensional spacetime coupled with an electromagnetic source is described by the action [52]

$$S = \frac{1}{16\pi G} \int dx^D \sqrt{-g} [R - F_{\mu\nu} F^{\mu\nu} + \alpha (R^2 - 4R_{\mu\nu} R^{\mu\nu} + R_{\mu\nu\beta\gamma} R^{\mu\nu\beta\gamma})], \quad (1)$$

where  $R$  is the scalar curvature, which corresponds to the well known Einstein-Hilbert contribution,  $R_{\mu\nu}$  and  $R_{\mu\nu\beta\gamma}$  are the Ricci and Riemann tensors respectively,  $\alpha$  is known as the GB coupling constant and  $F_{\mu\nu}$  is the electromagnetic tensor given by

$$F_{\mu\nu} = \partial_\mu A_\nu - \partial_\nu A_\mu, \quad (2)$$

with  $A_\mu$  being the quadripotential.  $\alpha$  has dimensions of [length<sup>2</sup>] and some authors take it between  $-8M^2 < \alpha < M^2$  [30]. Nevertheless, it is usual to consider the simple constrain  $\alpha > 0$  [17], since it has been shown that for  $\alpha < 0$  the BH solution might not be valid for small distances [40]. In this work, we will use the assumption  $\alpha > 0$ .

EGB gravity describes quadratic corrections to the curvature tensors from Lovelock's gravitational theory, but is also obtained in the low-energy limit of string theory, in which  $\alpha$  can be interpreted as the inverse stress of the string and is defined only with positive values [40]. Actually, the BH solution in EGB theory has already been deduced from various modified gravity theories. It was initially obtained in 1985 by Boulware and Deser in [2] for the cases where  $D \geq 5$ , since the GB term does not contribute to the gravitational dynamics

when  $D = 4$ . Then, Tomozawa in 2011 [3], through a regularization procedure, found that there could be, from a quantum perspective, a non-trivial contribution of the GB term to space-time in the case where  $D = 4$ . Later in 2013, Cognola et al. [4], through another process of regularization to EGB gravity, managed to perform a dimensional reduction under the Lagrangian formulation, finding again the BH type solution for the case in which  $D = 4$ . According to Lovelock’s theorem, the gravity of EGB is only introduced in cases where  $D > 4$  because, for smaller dimensions, the term with the GB coupling would not contribute dynamically [5]. In 2020, Glavan and Lin [6] used this formalism to obtain the same BH solution in 4D EGB gravity by simply proposing a rescaling of  $\alpha$ . However, several studies have shown that this previous proposal is problematic. This is easily suspected by the fact that the lagrangian action diverges and is not well-defined in the 4-dimensional limit, disregarding Lovelock’s theorem [1, 8–10]. Consequently, it has been clarified that the BH solutions of 4D EGB can be obtained from different approaches and theories of modified gravity that are well-defined. Therefore, it is not an entirely novel solution. To obtain coherent versions of the theory of BH solutions in 4D EGB gravity, alternative regularization processes have been applied. These include scalar-tensor theories from conformal regularizations [14, 15], the Kaluza-Klein regularized reduction [13], and other formalisms related to theories of gravity such as semi-classical or higher dimensional [1, 11, 12, 16, 17]. Taking this into account, we will study the solution of 4D EGB BHs within the context of consistent theories. For example, in [16], the suggested approach have two dynamical degrees of freedom by breaking the temporal diffeomorphism invariance and are explored in the context of EGB gravity in  $D = d + 1$  using the ADM decomposition. This undoubtedly shows that this BH solution has been of great interest in recent years. The spacetime under consideration is assumed to be static and spherically symmetric, and is described by

$$ds^2 = - f(r) dt^2 + f(r)^{-1} dr^2 + r^2 d\Omega_D^2, \tag{3}$$

where, if  $D = 4$ , we have that  $d\Omega_D^2 \equiv d\theta^2 + \sin^2\theta d\phi^2$  and

$$A_\mu = -\frac{Q}{r} dt, \tag{4}$$

so the solution of an electrically charged BH in 4D EGB gravity will take the form [52]

$$f^{(CEGB)}(r) = 1 + \frac{r^2}{2\alpha} \left[ 1 - \sqrt{1 + 4\alpha \left( \frac{2M}{r^3} - \frac{Q^2}{r^4} \right)} \right]. \tag{5}$$

This solution was first introduced in [7], in addition to a coupling with anti-de Sitter space. The asymptotic behavior of this solution is

$$f^{(CEGB)}(r) = 1 - \frac{2M}{r} + \frac{Q^2}{r^2} + \frac{4M^2\alpha}{r^4} - \frac{4MQ^2\alpha}{r^5} + \mathcal{O}\left(\frac{1}{r^6}\right). \tag{6}$$

When only the first and second orders are considered in the series expansion, the solutions of GR are clearly revealed.

For simplicity, from now on, the spacetime that describes the background geometry of an electrically charged BH in 4D EGB gravity of (5) will be denoted as the CEGB BH solution.

### 2.2 Horizons and Particular Cases

The CEGB BH solution has two horizons, the internal (Cauchy) horizon,  $r_-$ , and the event horizon,  $r_+$ , which are located at

$$r_{\pm} = M \pm \sqrt{M^2 - Q^2 - \alpha}. \tag{7}$$

The corresponding behavior of  $r_{\pm}$  is shown in Fig. 1 for different values of  $Q$  and  $\alpha$ . There, the monotonic corrections on  $r_{\pm}$  are evident, at higher values of  $\alpha$  and  $Q$ , the value of  $r_+$  decreases while  $r_-$  increases. Thus, it is possible to obtain a suitable value of the parameters  $\alpha$  and  $Q$  for which  $r_-$  and  $r_+$  become a single degenerate horizon (with  $r_- = r_+ = M$ ). This particular case is known as the extreme BH type and it is obtained when

$$M = M_{ext} = \sqrt{Q^2 + \alpha}. \tag{8}$$

Thus, when  $M = M_{ext}$ , the function  $f^{(CEGB)}$  has only one real root (corresponding to the degenerate horizon). When  $M > M_{ext}$  the usual BHs solutions are obtained, with two real roots representing the two horizon as in (7). Taking  $M = 1$  and  $M > M_{ext}$ ,  $\alpha$  takes values in the range

$$0 < \alpha \leq 1 - Q^2. \tag{9}$$

From here it is clear that when  $Q \rightarrow 1$ , the parameter  $\alpha \rightarrow 0$ . On the other hand, when  $M < M_{ext}$  we have two complex root and the solution will represent a naked singularity.

The BH solution  $f^{(CEGB)}$ , contains various types of BHs as particular limiting cases. First, the Schwarzschild space-time is reached when  $Q \rightarrow 0$  and  $\alpha \rightarrow 0$ , obtaining

$$f^{(Sch)} = 1 - \frac{2M}{r}. \tag{10}$$

The Reissner-Nordström (RN) BH is achieved by taking  $\alpha \rightarrow 0$  in the solution  $f^{(CEGB)}$ ,

$$f^{(RN)} = 1 - \frac{2M}{r} + \frac{Q^2}{r^2}. \tag{11}$$

This metric describes the electrically charged BHs of the theory of GR and the horizons are given by

$$r_{\pm} = M \pm \sqrt{M^2 - Q^2}. \tag{12}$$

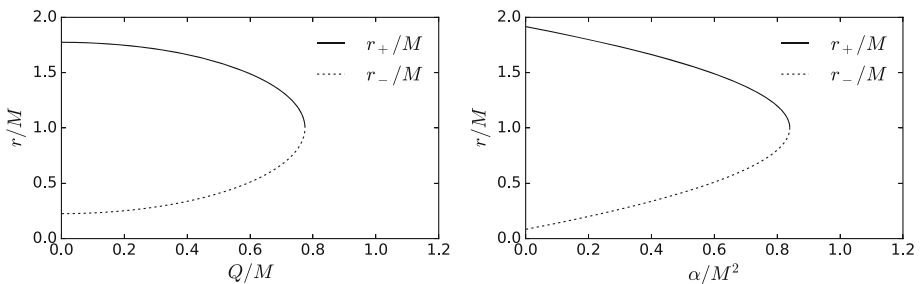


**Fig. 1** Radius of the event horizon  $r_+$  and of the inner horizon  $r_-$  for a CEGB BH. In the left panel it is shown in terms of the electric charge  $Q/M$  (using  $\alpha/M^2 = 0.1$ ) and in the right panel in terms of the GB coupling constant  $\alpha/M^2$  (with  $Q/M = 0.1$ )

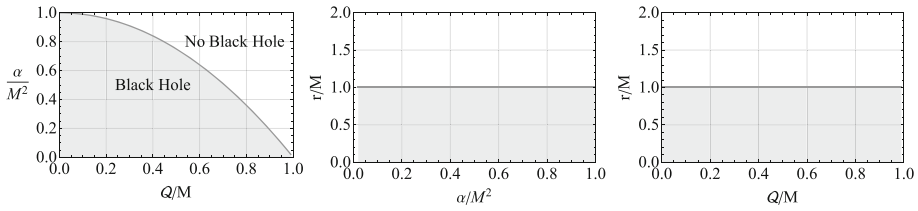


**Fig. 2** Dependences maximum values of GB constant and charge of the BH in 4D EGB gravity(left panel), event horizon to the maximum values of GB constant (middle panel), and event horizon to charge of the BH in 4D EGB gravity (right panel)

The third particular limiting case is the BH solution of 4D EGB gravity, obtained when  $Q \rightarrow 0$ ,

$$f^{(EGB)} = 1 + \frac{r^2}{2\alpha} \left( 1 - \sqrt{1 + \frac{8M\alpha}{r^3}} \right). \tag{13}$$

This spacetime has two real roots given by

$$r_{\pm} = M \pm \sqrt{M^2 - \alpha}. \tag{14}$$

Furthermore, we can determine the maximum values of the spacetime parameters by analyzing the spacetime to ensure that the BH possesses an event horizon. This can be achieved by solving the equations:

$$f^{(CEGB)}(r) = 0, \quad f^{(CEGB)'}(r) = 0 \tag{15}$$

where ' denotes the derivative with respect to the radial direction.

Figure 2 consists of three panels. The left panel illustrates the dependence of the maximum values of the GB constant and the charge of a black hole in 4D EGB gravity. The gray region represents black holes that possess an event horizon, while the white region corresponds to naked singularities, where there is no black hole at the center of our spacetime. Furthermore, the middle and right panels of Fig. 2 display an intriguing behavior of our event horizon, demonstrating that it remains constant regardless of changes in the parameters.

### 3 Quasinormal Modes of the Test Fields Perturbations

#### 3.1 Master Wave Equations of Scalar and Electromagnetic Fields

QNMs play an important role in investigating gravitational wave astronomy as they describe perturbations near BHs that can be observed through interferometry projects. The study of QNMs using various test fields, such as scalar, electromagnetic, and gravitational, provides valuable insights into the geometrical properties of BHs and helps determine their stability and uniqueness. To start the investigation, we propose examining the scalar and electromagnetic fields due to their relatively simple descriptions. Firstly, a massless scalar field,  $\Phi$ , is described by the Klein-Gordon equation that is written, using the background metric  $g_{\mu\nu}$ , as

$$\frac{1}{\sqrt{-g}} \partial_{\mu} (\sqrt{-g} g^{\mu\nu} \partial_{\nu} \Phi) = 0. \tag{16}$$

On the other hand, the electromagnetic field equation in a curved spacetime is

$$\frac{1}{\sqrt{-g}} \partial_\mu (\sqrt{-g} F^{\mu\nu}) = 0. \tag{17}$$

Using the formalism of perturbation theory and the scalar and vector harmonics to separate the spherical coordinates  $(t, r, \theta, \phi)$ , (16) and (17) can be transformed into a single general differential equation that adopts a Schrödinger-like form for stationary backgrounds [19, 53–55],

$$\frac{d^2 \Psi_s}{dr_*^2} + [\omega^2 - V_s(r)] \Psi_s = 0, \tag{18}$$

where we have introduced the well-known tortoise coordinate,  $r_*$ , defined by the relation

$$dr_* = \frac{dr}{f(r)} \tag{19}$$

and the effective potential takes de generalized form

$$V_s(r) = f(r) \left( \frac{\ell(\ell + 1)}{r^2} + \frac{(1 - s)}{r} f'(r) \right). \tag{20}$$

In this expression,  $s = 0$  and  $s = 1$  identify the scalar and the electromagnetic perturbations, respectively. Also, the prime denotes differentiation with respect to  $r$ , and  $\ell = 0, 1, 2, \dots$  are the multipole quantum numbers that come from spherical harmonic expansions.

The QNMs frequencies, denoted by  $\omega$  in (18), are obtained by requiring purely outgoing waves at infinity and purely incoming waves at the event horizon [30],

$$\Psi_s \sim \pm e^{\pm i\omega r_*}, \quad r_* \rightarrow \pm\infty. \tag{21}$$

In the case of the CEGB BH, the effective potential is always positive and have the shape of a potential barrier with a single peak. It also fulfills that

$$V_s^{(CEGB)}(r \rightarrow r_+) = V_s^{(CEGB)}(r \rightarrow \infty) = 0. \tag{22}$$

This behavior of the effective potential are the necessary boundary conditions to use the semi-analytical methods in the upcoming sections to calculate the QNMs frequencies.

### 3.2 The WKB Aproximation Method

Among the first theoretical approaches developed to calculate these QNMs frequencies in a semi-analytical manner is the well known Wentzel-Kramers-Brillouin (WKB) approximation method [56]. The derivation presented by Schutz and Will [56] begins with a series expansion of the redefined potential  $\Lambda(r_*) = \omega^2 - V_s(r_*)$ . The value of the turtle coordinate at which the maximum point of the effective potential is reached will be denoted by  $\tilde{r}_*$  and the potential evaluated at this point would be  $V_s(\tilde{r}_*) = V_0$ . Hence, the series expansion will be

$$\Lambda = \Lambda_0 + \frac{1}{2} \Lambda_0'' (r_* - \tilde{r}_*)^2 + \mathcal{O}(r_* - \tilde{r}_*)^3 + \dots \tag{23}$$

with  $\Lambda_0 = \omega^2 - V_0$  and  $\Lambda_0'' = -V_0''$ . It is clear that the second term of the expansion corresponds to the condition of the maximum point of the potential and therefore it vanishes. Substituting this expansion into the differential (18), the master wave equation reduces to the parabolic cylinder differential equation (usually called the Weber equation), which has



known solutions. Using the asymptotic behavior described above and imposing the boundary conditions that represent a BH, it is possible to find a simple analytical expression of the frequencies of the QNMs. At first order, it takes the form

$$\omega^2 = V_0 - i\sqrt{-2V_0''} \left( n + \frac{1}{2} \right). \tag{24}$$

where the expression is labeled with the harmonic or overtone number  $n$ . Both, the real part  $\omega_R$  and the imaginary part  $\omega_I$ , as well as the overtone number  $n$ , depend only on the maximum potential,  $V_0$ , and on the second derivative of the potential evaluated in the maximum point,  $V_0''$ . It should be noted that although the WKB formula has been derived analytically, it is not always possible to find the value of  $\tilde{r}_*$  explicitly. Therefore, it could be said that the WKB approach is a semi-analytic methodology. When this method was introduced, the QNMs of the gravitational perturbations of the Schwarzschild BH were estimated with an error of approximately 6% [56, 57].

In 1987, Iyer and Will [58] extended the WKB approximation method up to the  $3^{rd}$  order, improving the precision of the method up to an estimated error of less than 1% for  $n = 0$  [57]. The formula for the frequencies of the QNMs of the  $3^{rd}$  order of the WKB method is

$$\omega^2 = \left[ V_0 + \sqrt{-2V_0''}\tilde{\Gamma}_1 \right] - i\tilde{\Lambda}\sqrt{-2V_0''}[1 + \tilde{\Gamma}_2], \tag{25}$$

where  $\tilde{\Gamma}_1$  and  $\tilde{\Gamma}_2$  (can be consulted in [58]) give additional contributions that depend on  $n$  and on higher-order derivatives of the potential evaluated at the radial coordinate of the maximum point.

In 2003, Konoplya [59] extended the WKB method to  $6^{th}$  order, giving more accurate results than the previous expressions [57]. In this case, the frequencies are given by the relation

$$\frac{i(\omega^2 - V_0)}{\sqrt{-2V_0''}} - \sum_{j=2}^6 \Gamma_j = n + \frac{1}{2}, \tag{26}$$

where  $\Gamma_j$  (can be consulted in [59]) represent the higher-order contributions. This equation depends on terms up to  $V_0^{(12)}$ , that is, the twelfth derivative of the potential evaluated at the radial coordinate of the maximum point.

Finally, in 2017, Matyjasek and Opala [60] developed the extension of the WKB method up to  $13^{th}$  order. However, it has been shown that convergence in each order is not guaranteed and that the inclusion of more orders in the expansion does not ensure more accurate results [57]. In any case, the equations of the WKB method at  $1^{st}$ ,  $3^{rd}$  and  $6^{th}$  order give satisfactory results as long as  $\ell > n$ , with the best results obtained when  $\ell \gg n$  and acceptable results when  $\ell = n$  [57].

### 3.3 The Pöschl-Teller Potential Method

Another of the semi-analytical formalisms developed to calculate the frequencies of the QNMs of a BH was introduced in 1984 by Ferrari and Mashhoon [61]. It consists in an approximation the effective potential included in the (20) to the well known Pöschl-Teller potential, such that the master wave equation could be rewritten as

$$\frac{\partial^2 \Psi}{\partial r_*^2} + \left[ \omega^2 - \frac{V_0}{\cosh^2 \eta (r_* - \tilde{r}_*)} \right] \Psi = 0, \tag{27}$$

with

$$\eta^2 = \frac{V_0''}{2V_0}. \quad (28)$$

Making some substitutions and following a similar procedure as that in the WKB approximation, it is possible to transform (27) into a differential equation whose solutions are the hypergeometric functions [62]. Analyzing their asymptotic behavior, it is possible to develop a semi-analytic formula for the frequencies of QNMs,

$$\omega = \pm \sqrt{V_0 - \frac{\eta^2}{4}} - i\eta \left( n + \frac{1}{2} \right). \quad (29)$$

This approach considers both the real and imaginary components of the frequency to be dependent on the potential and its second derivative evaluated at the point of maximum. However, only the imaginary component,  $\omega_I$ , is affected by the overtone number,  $n$ . This method can provide more accurate results for  $\omega_I$  compared to those obtained using the WKB formula at 1<sup>st</sup> order of the (24). Hence, this treatment is not recommended for determining the real component  $\omega_R$  of the perturbation frequencies, except in specific cases such as the eikonal limit ( $\ell \rightarrow \infty$ ) or for the fundamental mode ( $n = 0$ ) [62]. In order to ensure greater precision in our discussions, in the upcoming sections we will keep these restrictions in mind and primarily focus on the eikonal QNMs of the fundamental mode ( $n = 0$ ).

In general, these semi-analytical formulas do not provide precise results when  $n \geq \ell$  or when the potential contains divergences, as is the case of perturbations of some massive scalar fields or for asymptotically deSitter and Anti-deSitter spaces. In these situations, the conditions required by the formalisms are not met, since they require the ability to identify the characteristic maximum point of the potential barrier. Consequently, other alternative approaches have been proposed for calculating QNM frequencies, including classical and numerical methods such as the Chandrasekhar-Detweiler method, direct integration of the wave equation, the Frobenius series method and its variations, the continued fractions method, and the monodromy technique for highly damped QNMs (for a discussion of these methods see [19, 62]). In recent years, novel and alternative computational methods have also been developed to obtain BH QNM frequencies, such as the Borel summation method [63], the Jansen Mathematica package [64] or the use of Neural Networks Methods [65].

## 4 Quasinormal Modes in the Eikonal Regime

### 4.1 Eikonal QNMs Approaches

The way in which light travels through space and interacts with matter and energy is one of the most fascinating aspects of the universe. Recently, a strong correlation between null geodesics and QNMs has been established [66]. Specifically, in the eikonal limit ( $\ell \rightarrow \infty$ ), the real and imaginary parts of QNMs frequencies for any spherically symmetric, asymptotically flat spacetime can be linked to the frequency and instability timescale of unstable circular null geodesics. This implies a connection between the possible paths of light rays and the response of the BH to external perturbations. Therefore, in the eikonal regime, we can establish a correlation between the radius of the photon sphere  $R_{ps}$  of a BH and its QNMs using the

following analytical expression [21, 51, 52, 67]

$$\omega = \Omega \ell - i \left( n + \frac{1}{2} \right) \lambda. \tag{30}$$

where  $\Omega$  is the angular velocity at the photon sphere,

$$\Omega = \sqrt{\frac{f'(R_{ps})}{2R_{ps}}}. \tag{31}$$

The symbol  $\lambda$  in (30) represents the Lyapunov exponent, which can be expressed as

$$\lambda = \sqrt{\frac{f(R_{ps}) \left( 2f(R_{ps}) - R_{ps}^2 f''(R_{ps}) \right)}{2R_{ps}^2}}. \tag{32}$$

This parameter is associated with the instability time scale of the photon sphere of a BH, indicating how quickly the orbit becomes unstable.

An interesting approach to the eikonal limit was proposed by M. Churilova [68] by noting that the effective potential  $V_{eik}$  in this limit does not usually depend on the spin of the field, except for some exceptions such as the backgrounds of charged BHs coupled to non-linear electromagnetic fields or the gravitational perturbations in some theories with higher curvature corrections, like EGB, Einstein-Lovelock or Einstein-dilaton-Gauss-Bonnet theories. Therefore, in most static and spherically symmetric spacetimes, the effective potential in the eikonal approximation for scalar and electromagnetic perturbations can be expressed as [68]

$$V_{eik}(r) = f(r) \left( \frac{\ell(\ell + 1)}{r^2} + \mathcal{O}(1) \right). \tag{33}$$

This means that the effective potential  $V_{eik}$  of the test fields perturbations in the eikonal limit can have the same form as the potential of the electromagnetic field perturbations  $V_{s=1}$ . We will analyze this fact below on the CEGB BH, with the help of our results of the QNMs frequencies of the scalar and electromagnetic field using high values of  $\ell$ .

Additionally, in [68] a general approach for eikonal QNMs of asymptotically flat BH solutions is presented. There, an expansion of the first order WKB formula of the (24) is written in powers of small parameters defined by the deviations of a given metric from the Schwarzschild one. These small parameters on the CEGB BH can be identified in the metric expansion of (6). Consequently, applying this Churilova analytical formula, in the eikonal limit, for a CEGB BH we obtain

$$\begin{aligned} \omega^{(Ch)} = & \frac{\ell + \frac{1}{2}}{3\sqrt{3}M} \left( 1 + \frac{Q^2}{6M^2} + \frac{2\alpha}{27M^2} - \frac{2Q^2\alpha}{81M^4} \right) \\ & - i \frac{\left( n + \frac{1}{2} \right)}{3\sqrt{3}M} \left( 1 + \frac{Q^2}{18M^2} - \frac{4\alpha}{27M^2} + \frac{22Q^2\alpha}{243M^4} \right) \\ & + \mathcal{O} \left( \frac{1}{\ell + \frac{1}{2}} \right). \end{aligned} \tag{34}$$

This result reproduces the analytical form of the eikonal QNMs of the 4D EGB BH found in [30], when  $Q/M = 0$ . Using (30) and (34) we have that the angular velocity of the photon

sphere is approximately

$$\Omega^{(Ch)} = \frac{(2\ell + 1) (162M^4 + 3M^2 (4\alpha + 9Q^2) - 4\alpha Q^2)}{972\sqrt{3}\ell M^5}, \tag{35}$$

and the Lyapunov exponent takes the form

$$\lambda^{(Ch)} = \frac{486M^4 + 9M^2 (3Q^2 - 8\alpha) + 44\alpha Q^2}{1458\sqrt{3}M^5}. \tag{36}$$

In the following sections, we will obtain the radius of the shadow of a CEGB BH from  $\omega^{(Ch)}$ . This approximate expression will not only depend on the geometric parameters of the BH solution, but also on  $\ell$ , so their applicability will be limited to the eikonal regime.

### 4.2 Eikonal QNMs of a CEGB BH

To calculate and study the eikonal QNMs of the CEGB BH, we use the WKB approximation formulas at 1<sup>st</sup>, 3<sup>rd</sup>, and 6<sup>th</sup> order, given by (24), (25), and (26), respectively. We also calculate the eikonal frequencies of the QNMs through the PT potential using (29), the eikonal formula given by the (30), and the Churilova’s analytical formula in (34). We show some of these results in Table 2 for the QNMs of scalar perturbations (s=0), in Table 3 for the QNMs of electromagnetic perturbations (s=1) and in Table 1 for both test fields.

In Table 1, we present the QNMs frequencies of the scalar and electromagnetic fields around a CEGB BH for  $\ell = 500000$  and various values of  $n$ . The second column summarizes the results obtained from the WKB method in three different orders and the PT method, which gave the same results. The third and fourth columns list the values calculated using the eikonal and Churilova formulas, respectively. It is evident that the real part of the frequencies does not depend on  $n$  in the eikonal regime. Additionally, it can be seen that the imaginary part of the frequencies obtained from the WKB and PT methods closely match the results calculated using the eikonal limit formula. Although Churilova’s eikonal formula is not as close to the other results, it still agrees well with them. Considering these facts, as depicted in Figs. 3 and 4, the curves representing the frequency behavior overlap in the solid line that summarizes

**Table 1** QNMs frequencies of the scalar and electromagnetic fields around a CEGB BH and for various values of  $n$ . (with  $\ell = 500000$ ,  $\alpha/M^2 = 0.1$  and  $Q/M = 0.1$ )

$n$	WKB 1 <sup>st</sup> , 3 <sup>rd</sup> and 6 <sup>th</sup> order and PT	Eikonal	Churilova
0	194248.7496-0.1896i	194248.5553-0.1896i	194191.8384-0.1897i
1	194248.7496-0.5687i	194248.5553-0.5687i	194191.8384-0.5692i
2	194248.7496-0.9478i	194248.5553-0.9478i	194191.8384-0.9486i
3	194248.7496-1.3270i	194248.5553-1.3270i	194191.8384-1.3281i
4	194248.7496-1.7061i	194248.5553-1.7061i	194191.8384-1.7075i
5	194248.7496-2.0853i	194248.5553-2.0853i	194191.8384-2.0870i
6	194248.7496-2.4644i	194248.5553-2.4644i	194191.8384-2.4664i
7	194248.7496-2.8435i	194248.5553-2.8435i	194191.8384-2.8458i
8	194248.7496-3.2227i	194248.5553-3.2227i	194191.8384-3.2253i
9	194248.7496-3.6018i	194248.5553-3.6018i	194191.8384-3.6047i

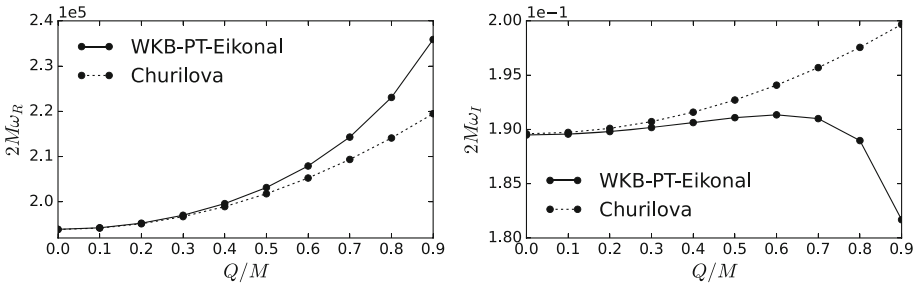


**Fig. 3** Eikonal QNMs frequencies for a CEGB BH depending on the electric charge  $Q/M$ . The left panel corresponds to the behavior of the real part of the frequencies while the right panel illustrates the behavior of the imaginary part. (using  $n = 0, \ell = 500000$  and  $\alpha/M^2 = 0.1$ )

the behavior of the WKB, PT and the eikonal methods, but differs from the dotted line that displays the results of the Churilova formula.

In Tables 2 and 3 we note that increasing  $\ell$  implies that these methods consistently yield similar values. It is also clear that the imaginary part of the frequencies does not depend on  $\ell$ , as is foreseen by the analytical expressions of the eikonal limit and Churilova formulas in (30) and (34), respectively.

For a CEGB BH, exactly the same values of the frequencies  $\omega$  are obtained in all the methods when  $\ell > 50000$  for the perturbations of both the scalar and the electromagnetic field. For the eikonal and Churilova formulas, this is an obvious result because they do not depend on the field. However, this result for the WKB and PT methods proves the convergence of the eikonal QNMs frequencies. Therefore, the effective potential of these test fields over the CEGB BH effectively behaves like (33) in the eikonal limit.

Similarly, our results for the WKB and PT methods when  $\ell < 50000$  show that the real and imaginary parts of the frequencies  $\omega$  are, in general, a little smaller for the electromagnetic field than for the scalar field, but they converge for  $\ell \approx 50000$ , as illustrated in Table 1.

Taking  $\omega = \omega_R - \omega_I$ , in Figs. 3 and 4, we show the effect of the geometric parameters  $Q$  and  $\alpha$  on the real and imaginary components of the eikonal QNMs frequencies for a CEGB BH. Our results show that, as the parameter  $\alpha$  increases, the real and imaginary part of the QNMs frequencies  $\omega_R$  and  $\omega_I$  increase monotonically as well. On the other hand, when the electric charge  $Q$  grows, the real part  $\omega_R$  also increases but the imaginary part of the frequencies increases up to a maximum peak of growth to decrease after it is reached. Our

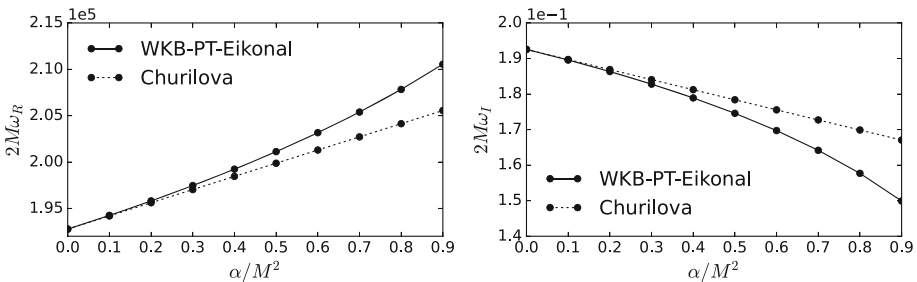


**Fig. 4** Eikonal QNMs frequencies for a CEGB BH depending on the GB coupling constant  $\alpha/M^2$ . The left panel corresponds to the behavior of the real part of the frequencies while the right panel illustrates the behavior of the imaginary part. (using  $n = 0, \ell = 500000$  and  $Q/M = 0.1$ )

**Table 2** QNMs frequencies of the scalar field ( $s=0$ ) around of a CEGB BH and for various high values of  $\ell$ . (with  $n = 0, \alpha/M^2 = 0.1$  and  $Q/M = 0.1$ )

$\ell$	WKB 1 <sup>st</sup> order	WKB 3 <sup>rd</sup> order	WKB 6 <sup>th</sup> order	PT	Eikonal	Churilova
5	2.1594-0.1895i	2.1390-0.1898i	2.1391-0.1898i	2.1426-0.1903i	1.9425-0.1896i	2.1361-0.1897i
10	4.0911-0.1896i	4.0804-0.1896i	4.0805-0.1896i	4.0823-0.1898i	3.8850-0.1896i	4.0780-0.1897i
50	19.6216-0.1896i	19.6194-0.1896i	19.6194-0.1896i	19.6197-0.1896i	19.4249-0.1896i	19.6134-0.1897i
100	39.0452-0.1896i	39.0441-0.1896i	39.0441-0.1896i	39.0443-0.1896i	38.8497-0.1896i	39.0325-0.1897i
500	194.4431-0.1896i	194.4428-0.1896i	194.4428-0.1896i	194.4429-0.1896i	194.2486-0.1896i	194.3858-0.1897i
1000	388.6915-0.1896i	388.6914-0.1896i	388.6914-0.1896i	388.6914-0.1896i	388.4971-0.1896i	388.5775-0.1897i
5000	1942.6798-0.1896i	1942.6798-0.1896i	1942.6798-0.1896i	1942.6798-0.1896i	1942.4856-0.1896i	1942.1106-0.1897i
10000	3885.1654-0.1896i	3885.1654-0.1896i	3885.1654-0.1896i	3885.1654-0.1896i	3884.9711-0.1896i	3884.0271-0.1897i
50000	19425.0498-0.1896i	19425.0498-0.1896i	19425.0498-0.1896i	19425.0498-0.1896i	19424.8555-0.1896i	19419.3586-0.1897i

**Table 3** QNMs frequencies of the electromagnetic field ( $s=1$ ) around of a CEGB BH and for various high values of  $\ell$ . (with  $n = 0, \alpha/M^2 = 0.2$  and  $Q/M = 0.2$ )

$\ell$	WKB 1 <sup>st</sup> order	WKB 3 <sup>rd</sup> order	WKB 6 <sup>th</sup> order	PT	Eikonal	Churilova
5	2.1646-0.1858i	2.1450-0.1859i	2.1451-0.1859i	2.1486-0.1865i	1.9687-0.1865i	2.1620-0.1873i
10	4.1338-0.1863i	4.1236-0.1863i	4.1236-0.1863i	4.1254-0.1865i	3.9374-0.1865i	4.1275-0.1873i
50	19.8840-0.1865i	19.8819-0.1865i	19.8819-0.1865i	19.8822-0.1865i	19.6872-0.1865i	19.8512-0.1873i
100	39.5713-0.1865i	39.5702-0.1865i	39.5702-0.1865i	39.5704-0.1865i	39.3744-0.1865i	39.5058-0.1873i
500	197.0691-0.1865i	197.0688-0.1865i	197.0688-0.1865i	197.0689-0.1865i	196.8722-0.1865i	196.7427-0.1873i
1000	393.9413-0.1865i	393.9411-0.1865i	393.9411-0.1865i	393.9412-0.1865i	393.7444-0.1865i	393.2889-0.1873i
5000	1968.9188-0.1865i	1968.9188-0.1865i	1968.9188-0.1865i	1968.9188-0.1865i	1968.7219-0.1865i	1965.6584-0.1873i
10000	3937.6407-0.1865i	3937.6407-0.1865i	3937.6407-0.1865i	3937.6407-0.1865i	3937.4439-0.1865i	3931.1203-0.1873i
50000	19687.4161-0.1865i	19687.4161-0.1865i	19687.4161-0.1865i	19687.4161-0.1865i	19687.2193-0.1865i	19654.8153-0.1873i

findings for the QNMs of the CEGB BH align with those reported in [52], where similar corrections due to  $Q$  and  $\alpha$  were observed. However, our analysis reveals that as  $Q$  increases,  $\omega_I$  also increases, until it reaches a value close to  $Q^2 = M^2 - \alpha$ , at which point  $\omega_I$  begins to decrease as depicted in Fig. 3. These same behaviors were observed in [61] for the QNMs of the RN BH due to electric charge, and in [69] for a charged BH in Einstein-Maxwell nonlinear electrodynamics. In the CEGB BH, the effects of electric charge on the QNMs are consistent with those reported in [46]. Furthermore, our results regarding the influence of the GB coupling constant  $\alpha$  on the real and imaginary parts of the QNMs of the CEGB BH are in agreement with the findings presented in [30, 34, 37, 46, 52].

Another interesting observation is that the QNMs frequencies calculated by the Churilova formula present a better agreement with other results in the literature when the geometric parameters of the BH are small. This is expected, given the nature of the solution’s expansion [68]. Therefore, the Churilova formula’s frequencies differ from other results as  $M$  approaches  $M_{ext}$ .

## 5 The Effective Potential and the Photon Sphere

### 5.1 The BH Photon Sphere Radius

The photon sphere, also known as the "light ring" or "photon orbit", for a static spherically symmetric BH is recognized as the orbit at which light moves in a unstable circular null geodesic. As mentioned in [21, 52], the Hamilton-Jacobi or Hamiltonian formulations can be used to find the equations of motion for photons around a static and spherically symmetric BH background and subsequently, permit to identify the effective potential that describes the system. From the critical point conditions of this potential, the radius of the photon sphere  $R_{ps}$  can be determined by solving the expression

$$2 - \frac{R_{ps} f'(R_{ps})}{f(R_{ps})} = 0. \tag{37}$$

Substituting the Schwarzschild metric on this expression, we obtain that

$$R_{ps}^{(Sch)} = 3M. \tag{38}$$

Using the solution of RN given by (11), we have

$$R_{ps}^{(RN)} = \frac{1}{2} \left( \sqrt{9M^2 - 8Q^2} + 3M \right) \tag{39}$$

It should be noted that this expression for  $R_{ps}^{(RN)}$  has the same analytical form given in [70] for the radial coordinate of the maximum of the corresponding effective potential of field perturbations in the eikonal limit. Additionally, the expression for  $R_{ps}^{(RN)}$  can be approximated for small values of  $Q$  as

$$R_{ps}^{(RN)} = 3M - \frac{2Q^2}{3M} - \frac{4Q^4}{27M^3} + O(Q^5). \tag{40}$$

Using the 4D EGB BH metric given by (13) in the condition of the (37), we get

$$R_{ps}^{(EGB)} = \frac{\left( M \left( \sqrt{16\alpha^2 - 27M^4 - 4\alpha} \right)^{2/3} + 3M^2 \right)}{\left( M \left( \sqrt{16\alpha^2 - 27M^4 - 4\alpha} \right) \right)^{1/3}}. \tag{41}$$



In [71], another alternative analytical expression is deduced for the radius of the photon sphere of the 4D EGB BH, with  $M = 1$ ,

$$R_{ps}^{(EGB)} = 2\sqrt{3} \cos\left(\frac{1}{3} \cos^{-1}\left(-\frac{4\alpha}{3\sqrt{3}}\right)\right). \tag{42}$$

Although we couldn't establish an equality between these two expressions, we have tested them numerically and they always gave identical results. However, both expressions lead to the same expansion,

$$R_{ps}^{(EGB)} = 3M - \frac{4\alpha}{9M} - \frac{8\alpha^2}{81M^3} + O(\alpha^3), \tag{43}$$

useful for small values of  $\alpha$ . Note that the expansions of  $R_{ps}^{(RN)}$  and  $R_{ps}^{(EGB)}$  show that the first term corresponds to radius of the photon spher for the Schwarzschild BH.

### 5.2 The Photon Sphere Radius for a CEGB BH

Using the expression of (37), an analytical expression for the radius of the photon sphere for a CEGB BH is obtained as

$$R_{ps}^{(CEGB)} = \frac{1}{2} \sqrt{-\frac{8M(2\alpha + 3Q^2)}{\sqrt{X}} - X + 18M^2} + \frac{\sqrt{X}}{2}, \tag{44}$$

$$X = \frac{27M^4 - 16Q^2(\alpha + Q^2)}{3^{1/3}Y} + \frac{Y}{3^{2/3}} + 6M^2 \tag{45}$$

$$Y = (-243M^6 + 72M^2(4\alpha^2 + 3Q^4 + 6\alpha Q^2) + Z)^{1/3}, \tag{46}$$

$$Z = \frac{1}{6} \sqrt{1728(27\alpha M^4 + 4Q^6)(64(\alpha + Q^2)^3 - 27M^4(4\alpha + 3Q^2))}. \tag{47}$$

The above equations for  $R_{ps}^{(CEGB)}$  effectively reproduce the analytic expressions corresponding to the radius of the photon spheres of the solutions of the particular limit cases. Taking  $Q \rightarrow 0$  and  $\alpha \rightarrow 0$ , we get  $R_{ps}^{(Sch)}$  in (38). Doing only  $\alpha \rightarrow 0$  gives  $R_{ps}^{(RN)}$  given by (39) and doing only  $Q \rightarrow 0$  recovers  $R_{ps}^{(EGB)}$  given by (41).

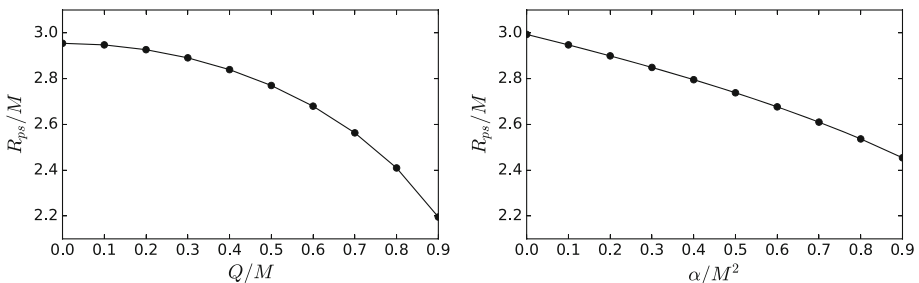


**Fig. 5** Photon sphere radius  $R_{ps}$  for a CEGB BH using the (47). In the left panel it is shown in terms of the electric charge  $Q/M$  (using  $\alpha/M^2 = 0.1$ ) and in the right panel in terms of the GB coupling constant  $\alpha/M^2$  (with  $Q/M = 0.1$ )

In Fig. 5, we show the effect of the geometric parameters  $Q$  and  $\alpha$  on  $R_{ps}^{(CEGB)}$ . It is clear that as both the electric charge and the GB coupling constant increase, the photon sphere radius becomes smaller. These results agree with those reported in [49, 71].

### 5.3 Correspondence Between Eikonal QNMs and Null Geodesics

As we stated above, there exist a correlation between null geodesics and eikonal QNMs frequencies for any spherically symmetric, asymptotically flat spacetime [66], which to a large extent can be linked to the fulfillment of the (30). However, with the simple fact that the BH solution is no longer valid for the WKB formula to first order, it is enough to believe that this connection does not hold. For example, the predicted correlation between null geodesics and QNMs is not upheld in the Einstein-Lovelock theory, as reported in [20], where authors showed that the radius of the photon sphere does not match the radial position of the extremum of the effective potential in the eikonal regime, contributing to the breakdown of the proposed correspondence. In the previous section, we found that the effective potential of perturbations of the scalar and electromagnetic fields around the CEGB BH follows (33) in the eikonal limit. However, this is not the case for gravitational perturbations in this background. In fact, in [30], it is shown that there is no correspondence between gravitational eikonal QNMs and null geodesics in the 4D EGB BH because of the form of the effective potential. They also mention that this correspondence does hold true for test fields perturbations when the background metric is considered to be a viable BH solution. Nevertheless, for scalar and electromagnetic fields in the CEGB BH spacetime, the QNMs calculations and its connections with the null geodesics and with the radius of the BH shadow should be satisfied and valid.

With the purpose of analyzing the correspondence in the CEGB BH, we will examine the agreement between the radius of the photon sphere,  $R_{ps}^{(CEGB)}$ , and the radial position of the maximum of the effective potential,  $\tilde{r}$ , for both scalar and electromagnetic field perturbations in the eikonal limit.

By differentiating with respect to the radial coordinate  $r$  and equating to zero the (20) of the effective potential,  $V_s(r)$ , gives a condition that find the radial coordinate  $\tilde{r}$  of the maximum point of the potential, as follows

$$0 = \frac{1}{r^3} \left\{ r f' [\ell(\ell + 1) + r(1 - s^2) f'] - f [2\ell(\ell + 1) + r(1 - s^2) (f' - r f'')] \right\}_{r=\tilde{r}}. \tag{48}$$

**Table 4** The effective potential and its radial coordinate of the maximum  $\tilde{r}$  for the scalar perturbations around a CEGB BH. We show the convergence for various values of  $\ell$ . (with  $\alpha/M^2 = 0.1$ ,  $Q/M = 0.1$  and  $R_{ps}^{(CEGB)} = 2.94761M$ )

$\ell$	$M^2 V_{s=0}$	$\tilde{r}/M$
5	1.15675	2.93786
10	4.17533	2.94489
50	96.24260	2.94749
100	381.12300	2.94758
500	9452.01630	2.94761
1000	37770.25849	2.94761
5000	943501.21847	2.94761
10000	3773627.47464	2.94761
50000	94333139.77196	2.94761

In Table 4, we present some values of the effective potential  $V_s$  for scalar perturbations and the radial position of the maximum  $\tilde{r}$  for various values of  $\ell$ , in a CEGB BH background. The results show that as  $\ell$  increases,  $V_s$  increases as well, but  $\tilde{r}$  becomes closer to the correct value of the radius of the photon sphere that, for the values  $\alpha/M^2 = 0.1$  and  $Q/M = 0.1$ , is  $R_{ps}^{(CEGB)} = 2.94761M$ . On the other hand, in the case of electromagnetic perturbations ( $s = 1$ ), the value of  $\tilde{r}$  can be found analytically and it exactly matches the expression for  $R_{ps}^{(CEGB)}$  given in (47). Consequently, this establishes that, in the eikonal limit, the CEGB BH also satisfies the connection between the maximum effective potential of the perturbations and the radius of the photon sphere, at least for scalar and electromagnetic fields.

## 6 The Black Hole Shadow

### 6.1 Connection Between Eikonal QNMs and the Radius of the BH Shadow

The BH shadow is a region of darkness that results from the deflection of light by the strong gravitational field in the BH surroundings. Light from background objects that would normally reach an observer is instead absorbed by the BH, resulting in the appearance of a shadow. The shape and size of this shadow is a unique characteristic of each BH and it depends on its geometric properties as well as on the characteristics of the material surrounding it.

Assuming a static observer positioned at a radial coordinate  $r_O$ , far enough from a spherically symmetric BH and such that  $f(r_O) \approx 1$ , the radius of the BH shadow,  $R_{sh}$ , as seen by this observer can be approximately calculated by [21, 30, 52, 54, 71]

$$R_{sh} \approx \frac{R_{ps}}{\sqrt{f(R_{ps})}}. \tag{49}$$

It can be shown that for a Schwarzschild BH, the shadow radius is  $R_{sh}^{(Sch)} = 3\sqrt{3}M$ . On the other hand, using the equation for  $R_{ps}^{(CEGB)}$  in terms geometric parameters for the CEGB BH solution to obtain the shadow radius is not straightforward. Therefore, in order to find an expression for  $R_{sh}^{(CEGB)}$ , we will use the previous calculation of the QNMs as the starting point. Based on the correlations between the distance from the BH and the behavior of eikonal QNMs with the photon sphere, it can be deduced that the real part of QNMs frequencies is inversely proportional to  $R_{sh}$  [21]. This relationship can be simply stated as follows

$$\omega_R = \lim_{\ell \gg 1} \frac{\ell}{R_{sh}}. \tag{50}$$

In general terms, it is also proposed that the relationship between the QNMs and the shadow radius of spherically symmetrical BHs can be expressed as [52]

$$\omega = R_{sh}^{-1} \left( \ell + \frac{D-3}{2} \right) - i \left( n + \frac{1}{2} \right) \lambda \tag{51}$$

where  $D$  represents the dimension of spacetime. In the eikonal limit, the term  $(D-3)/2$  can be disregarded. Nevertheless, it can be useful to assess the connection between BH shadows and QNMs at small  $\ell$ , especially in spherically symmetrical spacetimes defined in high or lower dimensions. Moreover, a generalized equation linking eikonal QNMs and shadows of rotating BHs is provided in [72]. Nonetheless, rotating BHs are not discussed in depth here but they hold significance for future related research projects.

### 6.2 CEGB BH Shadow Radius

The connection between the shadow and the QNMs of the massless scalar field around a CEGB BH is explored in [52], but they do it using only the 6<sup>th</sup> order WKB method and from the (51). In this work, we will use the (50), which holds only in the eikonal regime, and we will test several additional methods to study the shadow and QNMs of scalar and electromagnetic perturbations around a CEGB BH.

To determine the shadow radius of the CEGB BH, we use the frequencies of the QNMs computed through the WKB method at 1<sup>st</sup>, 3<sup>rd</sup>, and 6<sup>th</sup> order, as specified in (24), (25), and (26), respectively. We also use the frequencies of the QNMs derived from the PT potential method outlined in (29), the eikonal formula that linking QNMs with  $R_{ps}$  given by the (30), and the Churilova’s analytical formula presented in (34).

By substituting  $R_{ps}^{(CEGB)}$  from the (47) into the (49), it is possible to provide a rather complicated analytical expression of the shadow radius of CEGB BH, which is not shared here because it is so extensive. However, from Churilova’s analytical eikonal approach, contrary to all the others studied, it is possible to provide an approximate analytical formula for the CEGB BH shadow radius. Using the (34) and (50), it takes the form

$$R_{sh}^{(Ch)} = \frac{972\sqrt{3}\ell M^5}{(2\ell + 1)(162M^4 + 3M^2(4\alpha + 9Q^2) - 4\alpha Q^2)}. \tag{52}$$

This CEGB BH shadow radius formula is related to the eikonal limit and therefore, in addition to the geometric parameters of the solution, it also depends on  $\ell$ .

Using (49), a CEGB BH with  $\alpha/M^2 = 0.1$  and  $Q/M = 0.1$  has a shadow with radius  $R_{sh} = 5.14804M$ . In Table 5 we show the results obtained for the shadow radius for the CEGB BH for the fundamental mode ( $n = 0$ ) and using various values of  $\ell$ . There,  $R_{sh}^{(WKB-PT)}$  represents the shadow of the BH obtained from the WKB and PT potential methods,  $R_{sh}^{(Ei)}$  denotes the BH shadow radius obtained by using the eikonal equation and finally, the fourth column shows the results of Churilova’s analytical equation. It should be noted that  $R_{sh}^{(WKB-PT)}$  summarizes all the results of the WKB approximation methods at 1<sup>st</sup>, 3<sup>rd</sup> and 6<sup>th</sup> order and the PT potential because, as discussed in Table 1, these methods return the same values of the frequencies of the QNMs of the scalar and electromagnetic field in the eikonal limit. Therefore, as an initial conclusion of this work we see that all the

**Table 5** Shadow radius  $R_{sh}$  for a CEGB BH using various values of  $\ell$ . (with  $n = 0, \alpha/M^2 = 0.1, Q/M = 0.1$  and  $R_{sh} = 5.14804M$ )

$\ell$	$R_{sh}^{(WKB-PT)}/M$	$R_{sh}^{(Ei)}/M$	$R_{sh}^{(Ch)}/M$
5	4.63095	5.14804	4.68141
10	4.88864	5.14804	4.90434
50	5.09643	5.14804	5.09857
100	5.12227	5.14804	5.12393
500	5.14289	5.14804	5.14441
1000	5.14547	5.14804	5.14698
5000	5.14753	5.14804	5.14904
10000	5.14779	5.14804	5.14929
50000	5.14799	5.14804	5.14950
100000	5.14802	5.14804	5.14953
500000	5.14804	5.14804	5.14955

results obtained from the radius of its shadow show verify that the CEGB BH does indeed fulfill the connection between geometrical paramters and the QNMs. The results given by Churilova’s analytical eikonal approach show that  $R_{sh}^{(Ch)}$  achieves values that are very close to those obtained by the other approaches. For example, for  $\ell = 500000$  the deviation error between  $R_{sh}^{(WKB-PT)}$  and  $R_{sh}^{(Ch)}$  is less than 1%.

For practical purposes, doing  $\ell \rightarrow \infty$  removes the dependency on  $\ell$  from (52), simplifying the CEGB BH shadow radius to

$$R_{sh}^{(CEGB)} = \frac{486\sqrt{3}M^5}{162M^4 + 3M^2(4\alpha + 9Q^2) - 4\alpha Q^2} \tag{53}$$

From this expression, the shadow radius for the limiting paraticular cases of the CEGB BH can be calculated. For example, taking  $\alpha \rightarrow 0$  gives

$$R_{sh}^{(RN)} = \frac{18\sqrt{3}M^3}{6M^2 + Q^2}, \tag{54}$$

while taking  $Q \rightarrow 0$  produces

$$R_{sh}^{(EGB)} = \frac{81\sqrt{3}M^3}{27M^2 + 2\alpha}. \tag{55}$$

Similarly, by choosing  $Q \rightarrow 0$  and  $\alpha \rightarrow 0$  we recover the well-known limit of the Schwarzschild BH shadow radius,  $R_{sh}^{(Sch)} = 3\sqrt{3}M$ .

In Fig. 6, the solid line summarizes the BH shadow radius calculated using the QNMs given by the WKB-PT method and the eikonal limit formula while the dotted line shows the shadow radius from Churilova’s eikonal approach. It also illustrates the effects of the electric charge of the BH and the GB coupling constant on the shadow radius of a CEGB BH. As both parameters increase, the shadow radius decreases, which agrees with previous studies [34, 49, 52, 71]. This implies that, based on the range of possible values for the BH geometric parameters as stated in (9), the CEGB BH has a smaller shadow radius compared to the 4D EGB BH and the RN BH, and these BHs have a smaller shadow radius than that of a Schwarzschild BH

Figure 6 also show that the curves overlap for small values of  $\alpha$  and  $Q$  and then, in this region the CEGB BH shadow radius obtained from Churilova’s eikonal approach is very useful due to its analytical simplicity, providing accurate results.

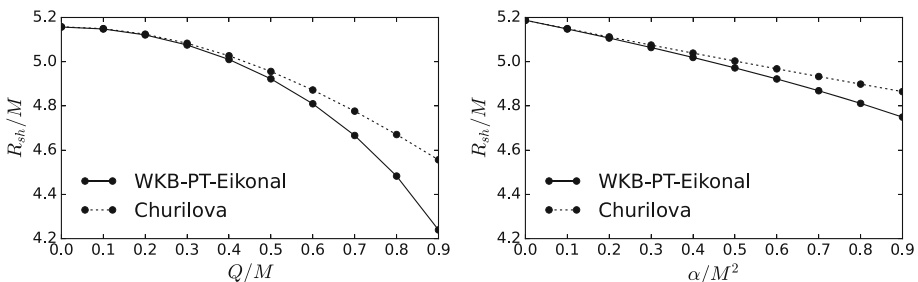


**Fig. 6** Shadow radius  $R_{sh}$  for a CEGB BH (with  $\ell = 500000$ ). In the left panel it is shown in terms of the electric charge  $Q/M$  (using  $\alpha/M^2 = 0.1$ ) and in the right panel in terms of the GB coupling constant  $\alpha/M^2$  (with  $Q/M = 0.1$ )

Ultimately, it is important to say that, in [71], the authors examine a hypothesis regarding a series of inequalities involving multiple parameters associated with the size of an 4D EGB BH. The proposal is that

$$\frac{3}{2}r_+ \leq R_{ps} \leq \frac{1}{\sqrt{3}}R_{sh} \leq 3M, \quad (56)$$

keeping in mind the ranges of (9) for the BH geometric parameters. We have evaluated the validity of this hypothesis involving the parameters that describe the size of a CEGB BH and our findings indicate that it satisfies the inequalities.

## 7 Conclusion

We have studied the relationship between the geometrical properties of a CEGB BH solution and the radius of the photon sphere, shadow radius, and eikonal QNMs. We obtained that the WKB method and PT potential method give the same results for eikonal QNMs for scalar and electromagnetic field perturbations of a CEGB BH. Our findings indicate that the real part of the eikonal QNMs frequencies is linked to the unstable circular null geodesic and shadow radius of a CEGB BH. We have illustrated how the parameters of electric charge  $Q$  and GB constant  $\alpha$  affect the QNMs frequencies, photon sphere, and shadow radius. Our results indicate that the real part of QNMs, photon sphere, and shadow radius are lower in CEGB BHs compared to those in 4D EGB, RN, and Schwarzschild BHs. Various equations have been derived for the radius of the photon sphere and shadows of BH solutions. Our investigation has shown that the eikonal approach proposed by Churilova provides a practical and straightforward approximate equation for the CEGB BH shadow radius, which is useful for small values of the geometric parameters. This approach facilitates analytical investigations, such as the study of astrophysical BH shadows, and could aid in observational investigations of QNMs in future gravitational wave projects.

There are several topics for future research related to this work. The following projects could be related to extending the analytical approach of the eikonal QNMs realized by Churilova to other BH solutions to test its methodology, including in spacetime arrangements that are not limited to being static, spherically symmetrical, or asymptotically flat. Moreover, the study of the spectrum of QNMs of CEGB BHs excited by an external source, such as an extreme mass ratio inspiral, could be explored. Additionally, the connections between the photon sphere, BH shadow, and eikonal QNMs should be explored for more realistic CEGB BHs or those related to alternative gravity theories. A particularly important BH solution to test these connections is the rotating CEGB BH, as recent theories also suggest connections between photon orbits, shadow radius, and eikonal QNMs in rotating BH solutions [72–74]. In [40], it was shown that the shadow of a rotating 4D EGB BH aligns with the M87\* BH shadow observed by the Event Horizon Telescope. Here, for a spin parameter of  $a = 0.1M$ , the GB coupling constant must be  $\alpha \leq 0.00394M^2$  (a very small value for  $\alpha$  which matches a good approximation of Churilova's eikonal approach). Therefore, it would be beneficial to also provide an analytical approach to these problems, linking the eikonal QNMs to the geometric properties of rotating CEGB BHs.

**Acknowledgements** We would like to thank Farrux Abdulxamidov for the support and the valuable discussions. We acknowledge partial financial support from Dirección de Investigación-Sede Bogotá, Universidad Nacional de Colombia (DIB-UNAL) under HERMES Project No. 57057 and Grupo de Astronomía, Astrofísica y Cosmología-Observatorio Astronómico Nacional.

**Funding** Open Access funding provided by Colombia Consortium.

**Open Access** This article is licensed under a Creative Commons Attribution 4.0 International License, which permits use, sharing, adaptation, distribution and reproduction in any medium or format, as long as you give appropriate credit to the original author(s) and the source, provide a link to the Creative Commons licence, and indicate if changes were made. The images or other third party material in this article are included in the article's Creative Commons licence, unless indicated otherwise in a credit line to the material. If material is not included in the article's Creative Commons licence and your intended use is not permitted by statutory regulation or exceeds the permitted use, you will need to obtain permission directly from the copyright holder. To view a copy of this licence, visit <http://creativecommons.org/licenses/by/4.0/>.

## References

1. Fernandes, P.G.S., Carrilho, P., Clifton, T., Mulryne, D.J.: The 4D Einstein-Gauss-Bonnet Theory of Gravity: A Review. *Class. Quantum Gravity* **39**, 063001 (2022). <https://doi.org/10.1088/1361-6382/ac500a>
2. Boulware, D.G., Deser, S.: String-Generated Gravity Models. *Phys. Rev. Lett.* **55**, 2656 (1985). <https://doi.org/10.1103/PhysRevLett.55.2656>
3. Tomozawa, Y.: Quantum Corrections to Gravity. (2011). <https://doi.org/10.48550/arXiv.1107.1424>
4. Cognola, G., Myrzakulov, R., Sebastiani, L., Zerbini, S.: Einstein Gravity with Gauss-Bonnet Entropic Corrections. *Phys. Rev. D* **88**, 024006 (2013). <https://doi.org/10.1103/PhysRevD.88.024006>
5. Bousder, M., El Bourakadi, K., Bennai, M.: Charged 4D Einstein-Gauss-Bonnet Black Hole: Vacuum Solutions, Cauchy Horizon. Thermodynamics. *Phys. Dark Universe* **32**, 100839 (2021). <https://doi.org/10.1016/j.dark.2021.100839>
6. Glavan, D., Lin, C.: Einstein-Gauss-Bonnet Gravity in Four-Dimensional Spacetime. *Phys. Rev. Lett.* **124**, 81301 (2020). <https://doi.org/10.1103/PhysRevLett.124.081301>
7. Fernandes, P.G.S.: Charged Black Holes in AdS Spaces in 4D Einstein Gauss-Bonnet Gravity. *Phys. Lett. B* **805**, 135468 (2020). <https://doi.org/10.1016/j.physletb.2020.135468>
8. Gürses, M., Şişman, T.Ç., Tekin, B.: Comment on "Einstein-Gauss-Bonnet Gravity in Four-Dimensional Spacetime." *Phys. Rev. Lett.* **125**, (2020). <https://doi.org/10.1103/PhysRevLett.125.149001>
9. Gürses, M., Şişman, T.Ç., Tekin, B.: Is There a Novel Einstein-Gauss-Bonnet Theory in Four Dimensions? *Eur. Phys. J. C* **80**, (2020). <https://doi.org/10.1140/epjc/s10052-020-8200-7>
10. Arrechea, J., Delhom, A., Jiménez-Cano, A.: Comment on "Einstein-Gauss-Bonnet Gravity in Four-Dimensional Spacetime," *Phys. Rev. Lett.* **125**, (2020). <https://doi.org/10.1103/PhysRevLett.125.149002>
11. Cai, R.G., Caob, L.M., Ohtab, N.: Black Holes in Gravity with Conformal Anomaly and Logarithmic Term in Black Hole Entropy. *J. High Energy Phys.* **2010**, (2010). [https://doi.org/10.1007/JHEP04\(2010\)082](https://doi.org/10.1007/JHEP04(2010)082)
12. Cai, R.G.: Thermodynamics of Conformal Anomaly Corrected Black Holes in AdS Space. *Phys. Lett. Sect. B Nucl. Elem. Part. High-Energy Phys.* **733**, (2014). <https://doi.org/10.1016/j.physletb.2014.04.044>
13. Lü, H., Pang, Y.: Horndeski Gravity as  $D \rightarrow 4$  Limit of Gauss-Bonnet. *Phys. Lett. B* **809**, 135717 (2020). <https://doi.org/10.1016/j.physletb.2020.135717>
14. Hennigar, R.A., Kubizňák, D., Mann, R.B., Pollack, C.: On Taking the  $D \rightarrow 4$  Limit of Gauss-Bonnet Gravity: Theory and Solutions. *J. High Energy Phys.* **2020**, (2020). [https://doi.org/10.1007/JHEP07\(2020\)027](https://doi.org/10.1007/JHEP07(2020)027)
15. Fernandes, P.G.S., Carrilho, P., Clifton, T., Mulryne, D.J.: Derivation of Regularized Field Equations for the Einstein-Gauss-Bonnet Theory in Four Dimensions. *Phys. Rev. D* **102**, 024025 (2020). <https://doi.org/10.1103/PhysRevD.102.024025>
16. Aoki, K., Gorji, M.A., Mukohyama, S.: A Consistent Theory of  $D \rightarrow 4$  Einstein-Gauss-Bonnet Gravity. *Phys. Lett. B* **810**, 135843 (2020). <https://doi.org/10.1016/j.physletb.2020.135843>
17. Ghosh, S.G., Singh, D.V., Kumar, R., Maharaj, S.D.: Phase Transition of AdS Black Holes in 4D EGB Gravity Coupled to Nonlinear Electrodynamics. *Ann. Phys.* **424**, 168347 (2021). <https://doi.org/10.1016/j.aop.2020.168347>
18. Kokkotas, K.D., Schmidt, B.G.: Quasi-Normal Modes of Stars and Black Holes. *Living Rev. Relativ.* **2**, (1999). <https://doi.org/10.12942/lrr-1999-2>
19. Konoplya, R.A., Zhidenko, A.: Quasinormal Modes of Black Holes: From Astrophysics to String Theory. *Rev. Mod. Phys.* **83**, 793 (2011). <https://doi.org/10.1103/RevModPhys.83.793>
20. Konoplya, R.A., Stuchlík, Z.: Are Eikonal Quasinormal Modes Linked to the Unstable Circular Null Geodesics? *Phys. Lett. B* **771**, 597 (2017). <https://doi.org/10.1016/j.physletb.2017.06.015>
21. Jusufi, K.: Quasinormal Modes of Black Holes Surrounded by Dark Matter and Their Connection with the Shadow Radius. *Phys. Rev. D* **101**, 084055 (2020). <https://doi.org/10.1103/PhysRevD.101.084055>
22. Liu, D., Yang, Y., Övgün, A., Long, Z.W., Xu, Z.: Gravitational ringing and superradiant instabilities of the Kerr-like black holes in a dark matter halo. *Eur. Phys. J. C* **83**, 565 (2023). <https://doi.org/10.1140/epjc/s10052-023-11739-w>



23. Li, P.C., Lee, T.C., Guo, M., Chen, B.: Correspondence of Eikonal Quasinormal Modes and Unstable Fundamental Photon Orbits for a Kerr-Newman Black Hole. *Phys. Rev. D* **104**, 084044 (2021). <https://doi.org/10.1103/PhysRevD.104.084044>
24. Bryant, A., Silva, H.O., Yagi, K., Glampedakis, K.: Eikonal Quasinormal Modes of Black Holes beyond General Relativity. III. Scalar Gauss-Bonnet Gravity. *Phys. Rev. D* **104**, 044051 (2021). <https://doi.org/10.1103/PhysRevD.104.044051>
25. Konoplya, R.A., Zinhailo, A.F., Stuchlík, Z.: Quasinormal Modes, Scattering, and Hawking Radiation in the Vicinity of an Einstein-Dilaton-Gauss-Bonnet Black Hole. *Phys. Rev. D* **99**, 124042 (2019). <https://doi.org/10.1103/PhysRevD.99.124042>
26. Glampedakis, K., Silva, H.O.: Eikonal Quasinormal Modes of Black Holes beyond General Relativity. *Phys. Rev. D* **100**, 044040 (2019). <https://doi.org/10.1103/PhysRevD.100.044040>
27. Liu, C., Zhu, T., Wu, Q., Jusufi, K., Jamil, M., Azreg-Aïnou, M., Wang, A.: Shadow and Quasinormal Modes of a Rotating Loop Quantum Black Hole. *Phys. Rev. D* **101**, 084001 (2020). <https://doi.org/10.1103/PhysRevD.101.084001>
28. Moura, F., Rodrigues, J.: Eikonal Quasinormal Modes and Shadow of String-Corrected d-Dimensional Black Holes. *Phys. Lett. B* **819**, 136407 (2021). <https://doi.org/10.1016/j.physletb.2021.136407>
29. Chen, C.Y., Chiang, H.W., Tsao, J.S.: Eikonal Quasinormal Modes and Photon Orbits of Deformed Schwarzschild Black Holes. *Phys. Rev. D* **106**, (2022). <https://doi.org/10.1103/PhysRevD.106.044068>
30. Konoplya, R.A., Zinhailo, A.F.: Quasinormal Modes, Stability and Shadows of a Black Hole in the 4D Einstein-Gauss-Bonnet Gravity. *Eur. Phys. J. C* **80**, (2020). <https://doi.org/10.1140/epjc/s10052-020-08639-8>
31. Zubair, M., Raza, M.A., Sarikulov, F., Rayimbaev, J.: “4D Einstein-Gauss-Bonnet Black Hole in Power-Yang-Mills Field: A Shadow Study.” [arXiv:2305.16888 [gr-qc]]
32. Zahid, M., Khan, S.U., Ren, J., Rayimbaev, J.: Geodesics and shadow formed by a rotating Gauss-Bonnet black hole in AdS spacetime. *Int. J. Mod. Phys. D* **31**(08), 2250058 (2022). <https://doi.org/10.1142/S0218271822500584>
33. Rayimbaev, J., Bardiev, D., Mirzaev, T., Abdurjabbarov, A., Khalmirzaev, A.: Shadow and massless particles around regular Bardeen black holes in 4D Einstein-Gauss-Bonnet gravity. *Int. J. Mod. Phys. D* **31**(07), 2250055 (2022). <https://doi.org/10.1142/S0218271822500559>
34. Liu, T.T., Zhang, H.X., Feng, Y.H., Deng, J.B., Hu, X.R.: Double Shadow of a 4D Einstein-Gauss-Bonnet Black Hole and the Connection between them with Quasinormal Modes. *Mod. Phys. Lett. A* **37**, (2022). <https://doi.org/10.1142/S0217732322501541>
35. Churilova, M.S.: Quasinormal Modes of the Dirac Field in the Consistent 4D Einstein-Gauss-Bonnet Gravity. *Phys. Dark Universe* **31**, 100748 (2021). <https://doi.org/10.1016/j.dark.2020.100748>
36. Zeng, X.X., Zhang, H.Q., Zhang, H.: Shadows and Photon Spheres with Spherical Accretions in the Four-Dimensional Gauss-Bonnet Black Hole. *Eur. Phys. J. C* **80**, 1 (2020). <https://doi.org/10.1140/epjc/s10052-020-08449-y>
37. Devi, S., Roy, R., Chakrabarti, S.: Quasinormal Modes and Greybody Factors of the Novel Four Dimensional Gauss-Bonnet Black Holes in Asymptotically de Sitter Space Time: Scalar, Electromagnetic and Dirac Perturbations. *Eur. Phys. J. C* **80**, (2020). <https://doi.org/10.48550/arXiv.2004.14935>
38. Övgün, A.: Black hole with confining electric potential in scalar-tensor description of regularized 4-dimensional Einstein-Gauss-Bonnet gravity. *Phys. Lett. B* **820**, 136517 (2021). <https://doi.org/10.1016/j.physletb.2021.136517>
39. Javed, W., Aqib, M., Övgün, A.: Effect of the magnetic charge on weak deflection angle and greybody bound of the black hole in Einstein-Gauss-Bonnet gravity. *Phys. Lett. B* **829**, 137114 (2022). <https://doi.org/10.1016/j.physletb.2022.137114>
40. Kumar, R., Ghosh, S.G.: Rotating Black Holes in 4D Einstein-Gauss-Bonnet Gravity and Its Shadow. *J. Cosmol. Astropart. Phys.* **2020**, 53 (2020). <https://doi.org/10.1088/1475-7516/2020/07/053>
41. Heydari-Fard, M., Heydari-Fard, M.: Null Geodesics and Shadow of 4D Einstein-Gauss-Bonnet Black Holes Surrounded by Quintessence. *Int. J. Mod. Phys. D* **31**, (2022). <https://doi.org/10.1142/S0218271822500663>
42. Kruglov, S.I.: Einstein-Gauss-Bonnet Gravity with Nonlinear Electrodynamics: Entropy, Energy Emission. Quasinormal Modes and Deflection Angle. *Symmetry*. **13**, 944 (2021). <https://doi.org/10.3390/sym13060944>
43. Churilova, M.S.: Quasinormal Modes of the Test Fields in the Consistent 4D Einstein-Gauss-Bonnet-(Anti)de Sitter Gravity. *Ann. Phys.* **427**, 168425 (2021). <https://doi.org/10.1016/j.aop.2021.168425>
44. Kumar, R., Islam, S.U., Ghosh, S.G.: Gravitational Lensing by Charged Black Hole in Regularized 4D Einstein-Gauss-Bonnet Gravity. *Eur. Phys. J. C* **80**(12), (2020). <https://doi.org/10.1140/epjc/s10052-020-08606-3>



45. Atamurotov, F., Shaymatov, S., Sheoran, P., Siwach, S.: Charged Black Hole in 4D Einstein-Gauss-Bonnet Gravity: Particle Motion, Plasma Effect on Weak Gravitational Lensing and Centre-of-Mass Energy. *J. Cosmol. Astropart. Phys.* **2021**, 045 (2021). <https://doi.org/10.1088/1475-7516/2021/08/045>
46. Zhang, C.Y., Zhang, S.J., Li, P.C., Guo, M.: Superradiance and Stability of the Regularized 4D Charged Einstein-Gauss-Bonnet Black Hole. *J. High Energy Phys.* **2020**, (2020). [https://doi.org/10.1007/JHEP08\(2020\)105](https://doi.org/10.1007/JHEP08(2020)105)
47. Zhang, M., Zhang, C.M., Zou, D.C., Yue, R.H.: Phase Transition and Quasinormal Modes for Charged Black Holes in 4D Einstein-Gauss-Bonnet Gravity. *Chinese Phys. C* **45**, (2021). <https://doi.org/10.1088/1674-1137/abe19a>
48. Papnoi, U., Atamurotov, F.: Rotating Charged Black Hole in 4D Einstein-Gauss-Bonnet Gravity: Photon Motion and Its Shadow. *Phys. Dark Universe* **35**, 100916 (2022). <https://doi.org/10.1016/j.dark.2021.100916>
49. Eslam Panah, B., Jafarzade, Kh., Hendi, S.H.: Charged 4D Einstein-Gauss-Bonnet-AdS Black Holes: Shadow, Energy Emission, Deflection Angle and Heat Engine. *Nucl. Phys. B* **961**, 115269 (2020). <https://doi.org/10.1016/j.nuclphysb.2020.115269>
50. Liu, P., Niu, C., Zhang, C.Y.: Instability of Regularized 4D Charged Einstein-Gauss-Bonnet de-Sitter Black Holes \*. *Chinese Phys. C* **45**, 025104 (2021). <https://doi.org/10.1088/1674-1137/abcd2d>
51. Mishra, A.K.: Quasinormal Modes and Strong Cosmic Censorship in the Regularised 4D Einstein-Gauss-Bonnet Gravity. *Gen. Relativ. Gravit.* **52**, (2020). <https://doi.org/10.1007/s10714-020-02763-2>
52. Chen, D., Gao, C., Liu, X., Yu, C.: The Correspondence between Shadow and Test Field in a Four-Dimensional Charged Einstein-Gauss-Bonnet Black Hole. *Eur. Phys. J. C* **81**, 700 (2021). <https://doi.org/10.1140/epjc/s10052-021-09510-0>
53. Baruah, A., Övgün, A., Deshamukhya, A.: Quasinormal Modes and Bounding Greybody Factors of GUP-corrected Black Holes in Kalb-Ramond Gravity. *Ann. Phys.* **455**, 169393 (2023). <https://doi.org/10.1016/j.aop.2023.169393>
54. Okyay, M., Övgün, A.: Nonlinear electrodynamics effects on the black hole shadow, deflection angle, quasinormal modes and greybody factors. *JCAP* **01**, 009 (2022). <https://doi.org/10.1088/1475-7516/2022/01/009>
55. Yang, Y., Liu, D., Övgün, A., Long, Z.W., Xu, Z.: Probing hairy black holes caused by gravitational decoupling using quasinormal modes and greybody bounds. *Phys. Rev. D* **107**, 064042 (2023). <https://doi.org/10.1103/PhysRevD.107.064042>
56. Schutz, B.F., Will, C.M.: Black Hole Normal Modes - A Semianalytic Approach. *Astrophys. J.* **291**, L33 (1985). <https://doi.org/10.1086/184453>
57. Konoplya, R.A., Zhidenko, A., Zinhailo, A.F.: Higher Order WKB Formula for Quasinormal Modes and Grey-Body Factors: Recipes for Quick and Accurate Calculations. *Class. Quantum Gravity* **36**, 155002 (2019). <https://doi.org/10.1088/1361-6382/ab2e25>
58. Iyer, S., Will, C.M.: Black-Hole Normal Modes: A WKB Approach. I. Foundations and Application of a Higher-Order WKB Analysis of Potential-Barrier Scattering. *Phys. Rev. D* **35**, 3621 (1987). <https://doi.org/10.1103/PhysRevD.35.3621>
59. Konoplya, R.A.: Quasinormal Behavior of the D-Dimensional Schwarzschild Black Hole and the Higher Order WKB Approach. *Phys. Rev. D* **68**, 24018 (2003). <https://doi.org/10.1103/PhysRevD.68.024018>
60. Matyjasek, J., Opala, M.: Quasinormal Modes of Black Holes: The Improved Semianalytic Approach. *Phys. Rev. D* **96**, 24011 (2017). <https://doi.org/10.1103/PhysRevD.96.024011>
61. Ferrari, V., Mashhoon, B.: New Approach to the Quasinormal Modes of a Black Hole. *Phys. Rev. D* **30**, 295 (1984). <https://doi.org/10.1103/PhysRevD.30.295>
62. Berti, E., Cardoso, V., Starinets, A.O.: Quasinormal Modes of Black Holes and Black Branes. *Class. Quantum Gravity* **26**, 163001 (2009). <https://doi.org/10.1088/0264-9381/26/16/163001>
63. Hatsuda, Y.: Quasinormal Modes of Black Holes and Borel Summation. *Phys. Rev. D* **101**, 24008 (2020). <https://doi.org/10.1103/PhysRevD.101.024008>
64. Jansen, A.: Overdamped Modes in Schwarzschild-de Sitter and a Mathematica Package for the Numerical Computation of Quasinormal Modes. *Eur. Phys. J. Plus* **132**, (2017). <https://doi.org/10.48550/arXiv.1709.09178>
65. Övgün, A., Sakalli, I., Mutuk, H.: Quasinormal Modes of DS and AdS Black Holes: Feedforward Neural Network Method. *Int. J. Geom. Methods Mod. Phys.* **18**, 2150154 (2021). <https://doi.org/10.1142/S0219887821501541>
66. Cardoso, V., Miranda, A.S., Berti, E., Witek, H., Zanchin, V.T.: Geodesic Stability, Lyapunov Exponents, and Quasinormal Modes. *Phys. Rev. D* **79**, 064016 (2009). <https://doi.org/10.1103/PhysRevD.79.064016>
67. Pantig, R.C., Mastrototaro, L., Lambiase, G., Övgün, A.: Shadow, lensing, quasinormal modes, greybody bounds and neutrino propagation by dyonic ModMax black holes. *Eur. Phys. J. C* **82**, 1155 (2022). <https://doi.org/10.1140/epjc/s10052-022-11125-y>

68. Churilova, M.S.: Analytical Quasinormal Modes of Spherically Symmetric Black Holes in the Eikonal Regime. *Eur. Phys. J. C* **79**, 629 (2019). <https://doi.org/10.1140/epjc/s10052-019-7146-0>
69. Panotopoulos, G., Rincón, Á.: Quasinormal Modes of Black Holes in Einstein-Power-Maxwell Theory. *Int. J. Mod. Phys. D* **27**, (2018). <https://doi.org/10.1142/S0218271818500347>
70. Konoplya, R.A., Stuchlík, Z., Zhidenko, A.: Massive Nonminimally Coupled Scalar Field in Reissner-Nordström Spacetime: Long-Lived Quasinormal Modes and Instability. *Phys. Rev. D* **98**, (2018). <https://doi.org/10.1103/PhysRevD.98.104033>
71. Guo, M., Li, P.C.: Innermost Stable Circular Orbit and Shadow of the 4D Einstein-Gauss-Bonnet Black Hole. *Eur. Phys. J. C* **80**, (2020). <https://doi.org/10.1140/epjc/s10052-020-8164-7>
72. Jusufi, K.: Connection between the Shadow Radius and Quasinormal Modes in Rotating Spacetimes. *Phys. Rev. D* **101**, 124063 (2020). <https://doi.org/10.1103/PhysRevD.101.124063>
73. Yang, H.: Relating Black Hole Shadow to Quasinormal Modes for Rotating Black Holes. *Phys. Rev. D* **103**, 084010 (2021). <https://doi.org/10.1103/PhysRevD.103.084010>
74. Li, P.C., Lee, T.C., Guo, M., Chen, B.: Correspondence of Eikonal Quasinormal Modes and Unstable Fundamental Photon Orbits for a Kerr-Newman Black Hole. *Phys. Rev. D* **104**, 084044 (2021). <https://doi.org/10.1103/PhysRevD.104.084044>

**Publisher's Note** Springer Nature remains neutral with regard to jurisdictional claims in published maps and institutional affiliations.